AFRL-RD-PS
TP-2009-1015

IMPACT OF RESOLUTION IN MULTI-CONJUGATE ADAPTIVE OPTICS SYSTEMS USING SEGMENTED MIRRORS: PREPRINT

Thomas A Corej
Jason D. Schmidt

1 June 2009

Technical Paper

AIR FORCE RESEARCH LABORATORY
Directed Energy Directorate
3550 Aberdeen Ave SE
AIR FORCE MATERIEL COMMAND
KIRTLAND AIR FORCE BASE, NM 87117-5776

REPORT DOCUMENTATION PAGE

Form Approved
OMB No. 0704-0188

1. REPORT DATE *(DD-MM-YYYY)*	2. REPORT TYPE	3. DATES COVERED *(From - To)*
01/06/2009	Technical Paper	June 1, 2009

4. TITLE AND SUBTITLE

Impact of resolution in Multi-Conjugate Adaptive Optics Systems Using Segmented Mirrors: Preprint

5a. CONTRACT NUMBER
N/A

5b. GRANT NUMBER
N/A

5c. PROGRAM ELEMENT NUMBER
N/A

6. AUTHOR(S)

Thomas A. Corej*; Jason D. Schmidt*

5d. PROJECT NUMBER
N/A

5e. TASK NUMBER
N/A

5f. WORK UNIT NUMBER
N/A

7. PERFORMING ORGANIZATION NAME(S) AND ADDRESS(ES)

Air Force Research Laboratory ***Air Force Institute of Technology**
3550 Aberdeen Ave SE **2950 Hobson Way**
Kirtland AFB, NM 87117 **Wright-Patterson AFB, OH 45433**

8. PERFORMING ORGANIZATION REPORT NUMBER

9. SPONSORING / MONITORING AGENCY NAME(S) AND ADDRESS(ES)

Air Force Research Laboratory
3550 Aberdeen Ave SE
Kirtland AFB NM 87117-5776

10. SPONSOR/MONITOR'S ACRONYM(S)
AFRL/RDSA

11. SPONSOR/MONITOR'S REPORT NUMBER(S)
AFRL-RD-PS-TP-2009-1015

12. DISTRIBUTION / AVAILABILITY STATEMENT

Approved for public release

13. SUPPLEMENTARY NOTES
Accepted for publication in the Optics and Photonics SPIE proceedings; 3-6 August 209; San Diego, CA. Public Release Approval 377ABW-2009-0835, 02 Jul 2009 "Government Purpose Rights"

14. ABSTRACT
In-moderate-to-strong scintillation, multi-conjugate adaptive optics (MCAO) may be able to compensate for amplitude and phase fluctuations. A MACO system is simulated with a segmented deformable mirror (DM) reshaping the amplitude and the second DM (continuous) flattening in the focal plane. A Gerchberg-Saxton (GS) type algorithm is used with Fresnel propagation between DM planes. The effects of varying the phase's apparent resolution on a Segmented DMI in the pupil plane is investigated. Results show the mean square area in the reshaped beam decreases as D/r 0 and Rytov number increase over the range of coherence diameter tested (0.11m-0.36m). The field-estimated Strehl ratio drops precipitously when the number of subapertures is increased beyond about 36 across, using a least-squares unwrapper, due to the presence of branch points. By using the mean of the DM2 phase within each subaperture before back propagating to the DM1 plane (inside the G-S loop), the Strehl ratio was improved 6-11 percent using 4-19 actuators across. A novel method of cascading segmented DMs, of increasingly higher resolution, doing amplitude reshaping followed by continuous DM to flatten the phase is explored.

15. SUBJECT TERMS
Gerchberg-Saxton Algorithm; Scintillation; Multi-Conjugate Adaptive Optics; Amplitude Reshaping; Resolution Effects; Branch Points/ Cuts

16. SECURITY CLASSIFICATION OF:			17. LIMITATION OF ABSTRACT	18. NUMBER OF PAGES	19a. NAME OF RESPONSIBLE PERSON
					Patrick Kelly
a. REPORT	b. ABSTRACT	c. THIS PAGE			19b. TELEPHONE NUMBER *(include area code)*
Unclassified	Unclassified	Unclassified	SAR	16	505- 846-2094

Standard Form 298 (Rev. 8-98)
Prescribed by ANSI Std. 239.18

Impact of Resolution in Multi-Conjugate Adaptive Optics Systems Using Segmented Mirrors

Thomas A. Corej and Jason D. Schmidt

Graduate School of Engineering, Air Force Institute of Technology, 2950 Hobson Way, Wright-Patterson AFB, OH 45433, USA;

ABSTRACT

In moderate-to-strong scintillation, multi-conjugate adaptive optics (MCAO) appears promising to compensate for amplitude and phase fluctuations. In this research, a MCAO system is simulated with a segmented deformable mirror (DM) reshaping the amplitude and the second DM (continuous) flattening the phase after propagation from the segmented mirror. A Gerchberg-Saxton (GS) type algorithm is used with Fresnel propagation between DM planes. The effects of varying the phase's apparent resolution on a segmented DM in the pupil plane is investigated. Results show the mean square error in the reshaped beam decreases as D/r_o and Rytov number increase over the range of conditions tested (r_o: 0.11 m - 0.36 m). The field-estimated Strehl ratio drops precipitously when the number of subapertures is increased beyond about 36 across, using a branch-point-tolerant unwrapper, due to the presence of branch points. On the second DM, by using the mean of the phase within each subaperture before back propagating to the first DM plane (inside the GS loop), the Strehl ratio was improved $6-11$ percent using $4-19$ actuators across. Further a novel method of cascading segmented DMs, of increasingly higher resolution, doing amplitude reshaping followed by a continuous DM to flatten the phase is explored.

Keywords: Gerchberg-Saxton algorithm, scintillation, multi-conjugate adaptive optics, amplitude reshaping, resolution effects, branch points/cuts

1. INTRODUCTION

Propagating light through the atmosphere with minimal distortion requires overcoming some of the challenges presented by atmospheric absorption/attenuation, refractive-index fluctuations, clouds, thermal blooming, etc to mitigate the atmosphere-induced angle-of-arrival variations, scintillation, phase fluctuations, etc. The refractivity fluctuations in the atmosphere are caused by variations in the temperature and pressure of pockets of air distributed throughout the atmosphere which vary primarily by altitude, time of day, location, and time of year.[1] The majority of the optical turbulence is located close to the ground, which is the main reason astronomical observatories are built at high altitudes (and at locations with generally clear skies).

Some of these effects can be mitigated through adaptive optics (AO) which typically make use of one or more natural or artificial beacons to sense and conjugate wavefront distortions. AO solutions typically involve some combination of wavefront sensor, computer, and a wavefront corrector. Usually, this involves correcting the phase fluctuations of the received wavefront to conjugate the effects of atmospheric turbulence. This is sufficient for many applications involving weak turbulence. However, for applications involving moderate-to-strong turbulence, scintillation becomes a significant factor that needs to be corrected as well to achieve a higher Strehl ratio or better resolution. Multi-conjugate AO (MCAO) is one solution originally proposed by Roggemann and Lee and further developed by Barchers and Ellerbroek.[2,3] This type of correction compensates both phase and amplitude fluctuations.

Continuous DMs have previously been studied for use in MCAO. Now, as segmented DM technology continues to improve with more actuators and higher fill factor, they are becoming suitable for MCAO. However, the size of each segment limits the resolution with which a wavefront can be corrected and/or a desired shape reproduced. This paper explores the effects of resolution on a MCAO system over a range of r_0's and Rytov numbers. This

Further author information: (Send correspondence to:)
Thomas A. Corej: E-mail: thomas.corej@afit.edu, Telephone: (937) 255-3636
Jason D. Schmidt, E-mail: jason.schmidt@afit.edu,Telephone: (937) 255-3636 x7224

paper also explores how resolution affects the ability to redistribute irradiance and the resolution at which branch points/cuts dominate the degradation in the Strehl ratio.

For this research, two DMs were used in computer simulation. The first DM was a phase-only segmented DM used to reshape a scintillated beam in an effort to make the amplitude uniform after a fixed near-field propagation distance. The second was a continuous DM attempting to flatten the phase of the light departing the second DM. The metric used to evaluate performance was the field-estimated Strehl ratio in conjunction with either a least-squares or least-squares principal-value phase unwrapper.[4] MCAO corrections can have applications in the areas of laser communication, high-power laser projection, and astronomical observations.

This rest of this paper is broken up into several sections. Section 2 describes the problem, some of the theory/models used to set up the simulation, and the parameters used in the simulation. Section 3 describes the beam-reshaping simulations. Section 4 presents the results of the computer simulations on resolution effects. It also briefly introduces a novel way of mitigating some branch points/cuts, and their detrimental effect on the Strehl ratio, by cascading DMs of increasing higher resolution via a mock 3-DM system. A summary of the results is given in Section 5 along with some suggested areas of further research.

2. MCAO PROBLEM DESCRIPTION, THEORY, AND SIMULATION SET UP

Based on other literature,[3,5,6] it is expected that a resolution will be reached beyond which the benefits gained by better phase control using smaller subapertures to gain a more uniform amplitude will be outweighed by branch points in the phase that degrade the Strehl ratio. The phase retrieval algorithm described here is based on the general G-S algorithm,[7–9] similarly modified by Barchers and Ellerbroek,[3] so that near-field propagation after DM1 provides the irradiance redistribution. However, unlike the approach of Barchers,[10] who used a Gaussian spatial filter on the phase commands on both DMs, a simpler technique of just using the mean of the DM2 phase within each respective subaperture was employed inside the G-S algorithm to achieve a higher Strehl ratio than using the unmodified G-S algorithm.

2.1 Problem Description

This research studies MCAO performance for light propagating through long, horizontal paths of atmospheric turbulence. The methodology is to use wave optics simulations with multiple phase screens to model the turbulence and representative models of the DMs. The simulation uses a point-source beacon, and the MCAO system seeks to improve images of the beacon. Figure 1 shows the general simulation set up for an imaging horizontal propagation constant C_n^2 scenario. Two phase screens are used to control the desired r_0 and σ_χ^2 values of the overall free space path length. Two DMs are used with the first controlling the amplitude and the second DM flattening the phase. A near-field Fresnel propagation distance is used between the two DMs similar to Barchers and Ellerbroek.[3] The resolution of each DM and the propagation distance between them are the main variables of this research.

This simulation modelled a horizontal propagation scenario which assumed a constant C_n^2 value. As a guide to determine the size of the aperture needed for a system, the coherence length r_0 is used here. For a laser communication type application, one of the primary variables to consider is the log-amplitude variance or Rytov number as a measure of the scintillation strength.[1] The spherical wave coherence length $r_{0,sp}$ and Rytov number σ_χ^2 value at each of the four turbulence conditions are shown in Table 1. These conditions would cause a typical single-DM AO system to fail as the Rytov number is increased.[2,5,11,12] An MCAO approach offers a potential solution. Table 1 includes the r_0 values ($r_{0,1}$ and $r_{0,2}$) for each phase screen and other key parameters of interest. A discussion on how these values were determined is covered in the next section under the layered turbulence model.

One of the main topics of this research is to determine if there was a limit beyond which going to a smaller size subapertures on a segmented DM was no longer beneficial. To investigate that, six different apparent resolutions were simulated: $4-5$ subapertures across, 9 subapertures across, $18-19$ subapertures across, $36-37$ subapertures across, 75 subapertures across, and 150 subapertures across in the DM1 plane as shown in Fig. 2. The effects of a segmented DM needed to be modelled. To adjust the resolution on the first DM (segmented DM), the phase was pixellated to give the same value of phase to all points within subapertures of various sizes as shown in Fig.

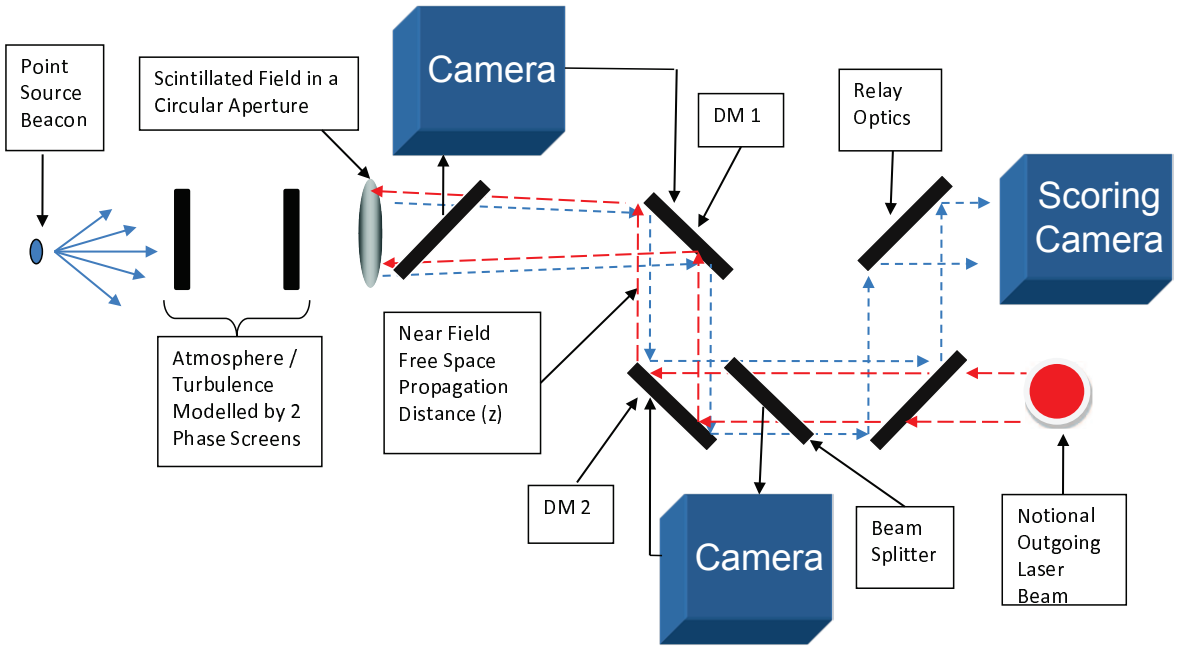

Figure 1. General MCAO Simulation Set Up

Table 1. Turbulence Conditions of Simulation and Phase Screen Values

C_n^2 [$m^{-2/3}$]	3.08×10^{-18}	1.5×10^{-17}	6.6×10^{-17}	1.1×10^{-16}	Phase Screen Location
$r_{0,1}$	0.3862	0.2324	0.1557	0.1162	$z_1 = L/4$
$r_{0,2}$	0.2882	0.1734	0.1162	0.0867	$z_2 = 3L/4$
σ_χ^2	0.1672	0.39	0.7599	1.2379	
$r_{0,sp}$ [m]	0.3632	0.2185	0.1464	0.1093	
θ_0 [μm]	1.1418	0.687	0.4604	0.3435	
Misc.	$L = 100$ km	$h = 12.19$ km	$A = 1.7 \times 10^{-14}$	$\lambda = 1.3$ μm	horizontal prop.

2. While it appears from Fig. 2 that having finer and finer control over the phase of each subaperture to control the amplitude of a propagated field is beneficial, it is shown later, in Figs. 4 and 5, the general resolution at which branch points in the DM2 field phase negate and further degrade the benefits of more finely controlling and reshaping the amplitude.

2.2 Overview of Layered Turbulence Model

For computer simulations, it is sometimes beneficial to use a finite number of discrete phase screens to each equivalently represent a much larger thickness of turbulence along the propagation path. Hence propagation is modelled as vacuum propagation from the source to the first phase screen (which models a certain thickness of turbulence) where the phase screen is applied, vacuum propagation to the next phase screen, and so on until the light reaches the receiver or target.[13] By modelling the turbulence as layers, it is then possible to set the overall values of r_0 and σ_χ^2 by varying the values of r_0 on each individual phase screen. For this simulation two phase screens are used at locations $L/4$ and $3L/4$, where L is the total free-space propagation distance.

For a spherical wave (denoted SP), the atmospheric coherence diameter and Rytov number are given by[1]

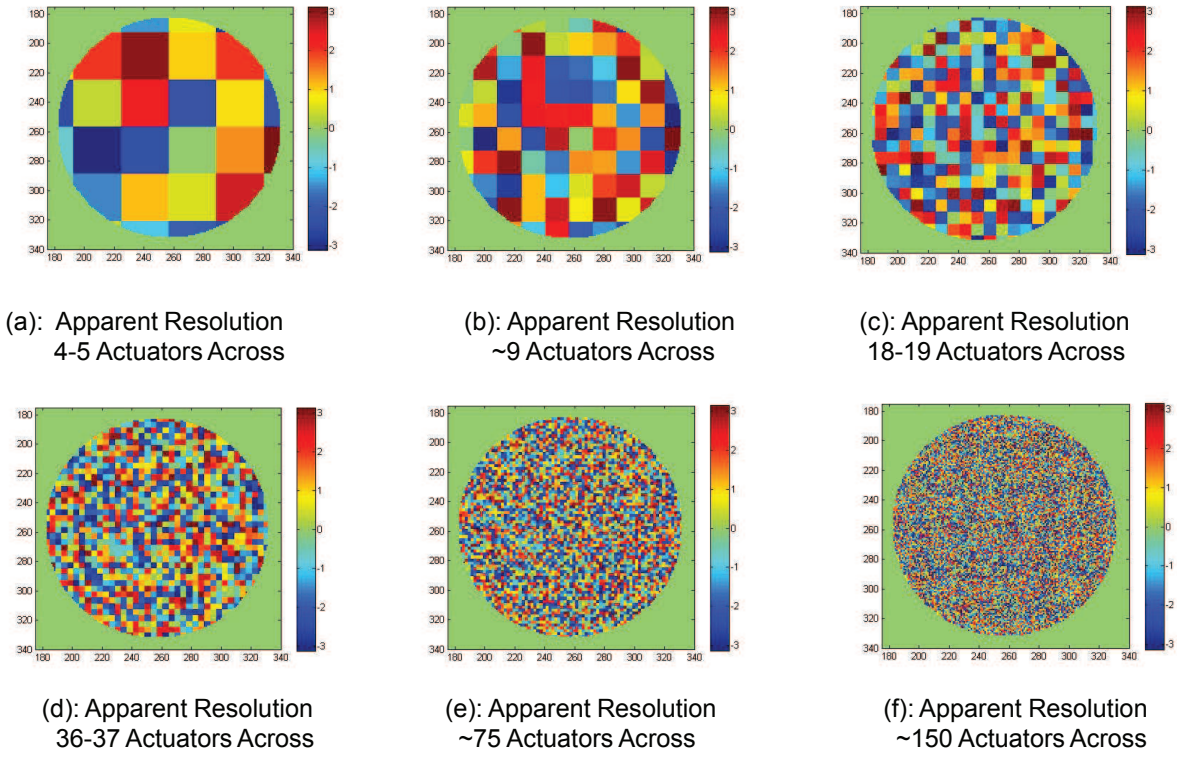

Figure 2. Typical Commands for a Segmented Mirror Model on DM1

$$r_{0,SP} = \left[0.423k^2 \int_0^L C_n^2(z) \left(\frac{z}{L}\right)^{\frac{5}{3}} dz\right]^{-3/5} \tag{1}$$

$$\sigma^2_{\chi,SP} = 0.5631\, k^{\frac{7}{6}} \int_0^L C_n^2(z) z^{\frac{5}{6}} (1 - z/L)^{\frac{5}{6}}\, dz. \tag{2}$$

To convert these equations to a layered model, the integral is replaced by a summation of the effective structure parameter $C^2_{n_i}$, the screen location z_i, and the thickness Δz_i of the turbulence represented by the i^{th} phase screen as

$$\int_0^L C_n^2(z)(z)^m dz = \sum_{i=1}^{N} C^2_{n_i} z_i^m \Delta z_i, \tag{3}$$

where z is a variable of integration, N represents the number of phase screens used, and m is the order of the moment.[12] Hence, the discrete sum versions of r_0 and σ^2_χ for a spherical wave can be written as

$$r_{0,SP} = \left[0.423\, k^2 \sum_{i=1} C^2_{n_i} (z_i/L)^{5/3} \Delta z_i\right]^{-3/5}, \tag{4}$$

$$\sigma^2_{\chi,SP} = 0.5631 k^{7/6} \sum_{i=1} C^2_{n_i} (z_i/L)^{5/6} (L - z_i)^{5/6} \Delta z_i. \tag{5}$$

However, the coherence diameter of each phase screen can be written as

$$r_{0_i} = [0.423\, k^2 C_{n_i}^2 \Delta z_i]^{-3/5}, \tag{6}$$

where the overall coherence diameter is $r_0 = \left(\sum_{i=1}^{N} r_{0_i}^{-5/3}\right)^{-3/5}$. The phase screens have no propagation and are treated such that the plane wave r_0 equations are used.[12,13] Using two phase screens yields

$$r_{0,SP}^{-5/3} = 0.423k^2 \left[C_{n_1}^2 (z_1/L)^{5/3} \Delta z_1 + C_{n_2}^2 (z_2/L)^{5/3} \Delta z_2\right], \tag{7}$$

$$\sigma_{\chi,SP}^2 = 0.5631k^{7/6} \left[C_{n_1}^2 (z_1/L)^{5/6} (L-z_1)^{5/6} \Delta z_1 + C_{n_2}^2 (z_2/L)^{5/6} (L-z_2)^{5/6} \Delta z_2\right], \tag{8}$$

where z_1 and z_2 represent the locations of the two phase screens relative to the source at $z = 0$, L is the total propagation distance, and Δz_1 and Δz_2 are the thickness of the atmosphere represented by phase screens 1 and 2 respectively.

To simplify the equations further to remove the $C_{n_i}^2$ and Δz_i terms, Eq. (7) for the coherence of the individual phase screens is used to obtain relations that depend solely on the r_0 values of the individual phase screens, the phase screen locations, and the total propagation distance L as

$$r_{0,SP}^{-5/3} = r_{0,1}^{-5/3} (z_1/L)^{5/3} + r_{0,2}^{-5/3} (z_2/L)^{5/3}, \tag{9}$$

$$\sigma_{\chi,SP}^2 = 1.3312k^{-5/6} \left[r_{0,1}^{-5/3} (z_1/L)^{5/6} (L-z_1)^{5/6} + r_{0,2}^{-5/3} (z_2/L)^{5/6} (L-z_2)^{5/6}\right]. \tag{10}$$

By picking z_1 and z_2 as some fraction of the total propagation distance L (i.e. $z_1 = L/2$), the dependence on L is removed as well for the $r_{0,i_{SP}}^{-5/3}$ term. With this technique, the locations of the phase screens can be fixed. Then to choose the overall value of r_0 and σ_χ^2, only the r_0 values of phase screens 1 and 2 need to be adjusted. For each atmosphere (specified by overall r_0 and σ_χ^2), Eqs. (9) and (10) were used to solve for $r_{0,1}$ and $r_{0,2}$ subject to the constraint that $r_{0,1}$ and $r_{0,2}$ must be real and positive. The phase screens were generated using the Fourier-series method introduced by Welsh[14] and developed by Magee.[15] Each phase screen was checked with the structure function, and the full path was checked with the degree of coherence compared with the theoretical results based on a layered turbulence model.[16]

2.3 Modelling a Point Source

To model a true point source, one would use a unit impulse or Dirac delta function.[17,18] However, one drawback of a point source for simulations with discrete samples on a finite grid is that the impulse function's Fourier spectrum has infinite spatial bandwidth. One way to get around the problem of the infinite spectral extent is to construct a model of the point source that mimics a point source that it is accurate over the grid boundaries (i.e. of limited angular extent).[13,19] For example, Martin and Flatté used a narrow Gaussian source.[19] This allows a point source to be modelled accurately over the grid boundaries or detector area, but with finite spatial extent and hence a finite number of samples can be used. The point source of finite spectral extent for this work was modelled as[13]

$$U_{pt}(x_1, y_1) = \exp\left[i\,\frac{k}{2\Delta z}(x_1^2 + y_1^2)\right] \left(\frac{D}{\lambda\,\Delta z}\right)^2 \operatorname{sinc}\left(\frac{D}{\lambda\,\Delta z} x_1\right) \operatorname{sinc}\left(\frac{D}{\lambda\,\Delta z} y_1\right), \tag{11}$$

where Δz is the propagation distance, x_1 and y_1 are source-plane coordinates, and D is the diameter of the observation plane's uniformly illuminated region.

2.4 Modelling Adaptive Optics

Using the techniques of Lukin,[20] DM1 was modelled as a segmented DM doing phase only (single degree of freedom) correction with square subapertures and 100 percent fill factor. The DM1 influence function for each subaperture is modelled as a rectangle.

As the apparent resolution of DM1 in the simulation changes, the number of grid points across the DM1 aperture also changes. At 512 points across the field (which includes zero padding), the number of subapertures across the received DM1 aperture equals 150 subapertures across. Likewise for 256, it corresponds to 75 subapertures across; for 128: 36-37 subapertures across; for 64: 18-19 subapertures across; for 32: about 9 subapertures across; and for 16: 4-5 subapertures across.

DM2 was modelled as a continuous facesheet. To account for the impact of adjoining actuators, an influence function is applied which essentially smoothes out the contributions of adjoining actuators. According to Lukin, Gaussian influence functions are representative of measured data from many typical continuous DMs.[20] Lukin's influence function is closer to that of Jagourel and Gafford,[21] or more simplified than the general higher order Gaussian function of Ealey and Wellman.[22] Lukin's form of the Gaussian influence function was used for this research: $f(\rho) = a\ \exp(-\rho^2/w^2)$ where ρ is the radial coordinate [i.e. $(x^2+y^2)^{1/2}$] and a is a scaling term set so that $f(\rho)$ integrates to 1. The number of neighboring pixels accounted for in the smoothing varies based on the halfwidth, w chosen for the Gaussian response function. The halfwidth usually "ranges from 0.7 to $0.8d$, where d is the spacing between actuators".[20] However, those number of subapertures across listed earlier do not match the number of subapertures/actuators typically found on deformable mirrors. As such, the following numbers of subapertures across were used for each given number of points across the field at DM2: for 512, 256, and 128: 30 subapertures across; for 64: 16 subapertures across; for 32: 8 subapertures across; and for 16: 3 subapertures across. Those correspond to continuous deformable mirrors with 30×30 actuators, 16×16 actuators, 8×8 actuators, and 3×3 actuators respectively on DM2 at those different respective apparent resolution levels.

2.5 Metrics

Strehl ratio is a common measure of imaging system performance and MSE is a common measure of beam reshaping performance. Similar to Barchers and Ellerbroek,[3] the metric used to evaluate the performance of the algorithm was the field-estimated Strehl ratio given by

$$S = \frac{\left|\int\int U_T U_E^* dxdy\right|^2}{\left|\int\int U_T U_T^* dxdy\right| \left|\int\int U_E U_E^* dxdy\right|} \tag{12}$$

where U_T is the true complex field (i.e. field of a vacuum propagated beacon) and U_E is the estimated complex field (i.e. reshaped DM2 field). Additionally, in some simulations, the mean square error (MSE) of the reshaped DM2 field was examined as an additional metric.

3. BEAM RESHAPING SIMULATIONS

Next the AO components were modelled. Now, operating the AO system requires some optimization of the G-S algorithm. To determine the number of iterations of the G-S type algorithm to use, simulations were conducted to plot the Strehl ratio (assuming perfect phase correction in the DM2 plane) versus MSE for 12 iterations at each apparent resolution level. Four realizations of the MCAO system are shown in Fig. 3 to give an idea of the spread and trend of MSE at each iteration number. Additionally, the points for the fourth realization were connected to illustrate the path the Strehl ratio follows and a single realization of a single-DM phase-only correction is included for comparison as shown in Fig. 3.

Note that for $4-5$ subapertures across, after about 3 iterations, due to the large size of subapertures and hence little control of the irradiance redistribution; further iterations result in decreased Strehl ratio as often as increased Strehl ratio. Contrast that with the case for 150 subapertures across, and the Strehl ratio is improved with each further iteration shown; although, the magnitude of the improvement is less and less for each additional iteration. Again, this assumes perfect phase correction on DM2 (and hence the effects of branch points are not accounted for on these plots). Based on these results, the number of iterations to use was set at 5 which generally

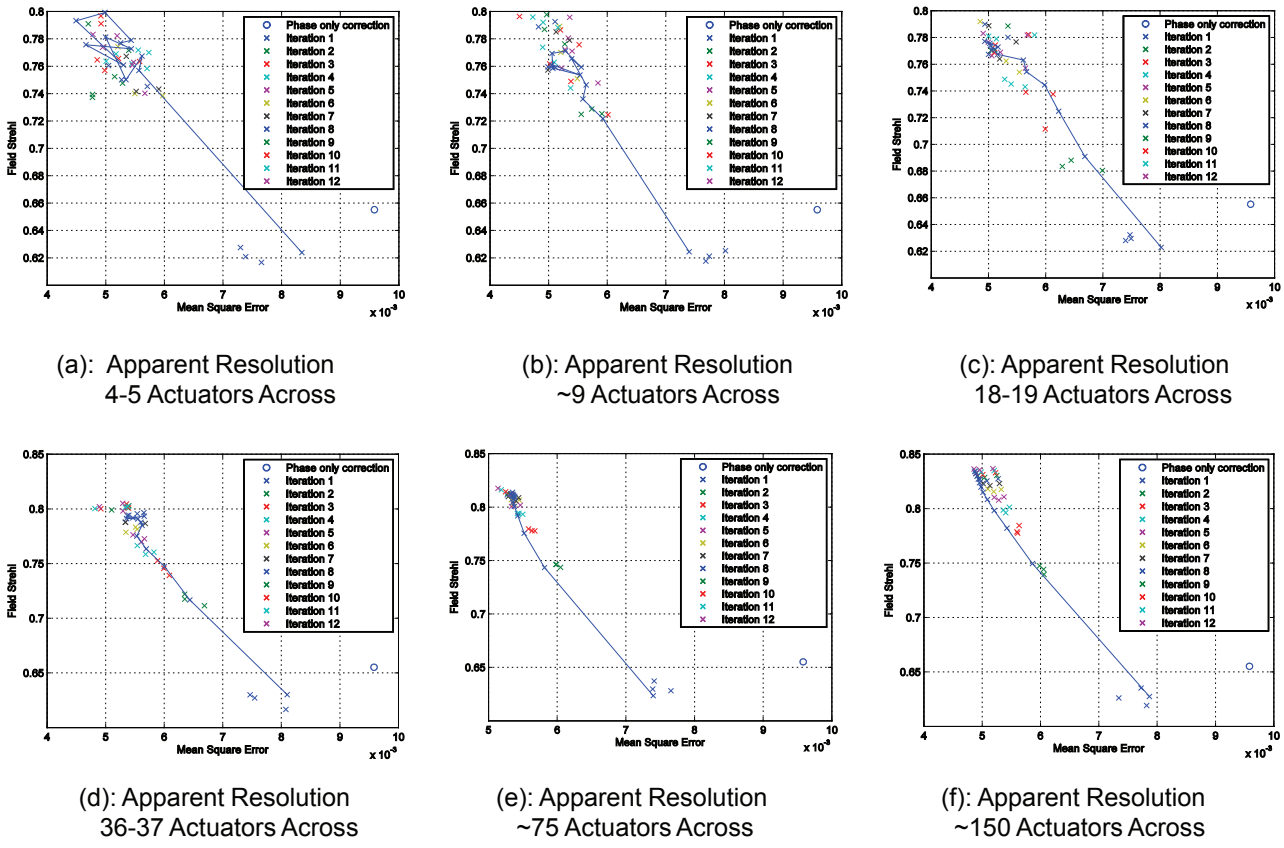

Figure 3. Strehl Ratio Vs. MSE Over Apparent Resolution Range

gave a Strehl ratio that was within 10 percent of the value that would have been achieved after 12 iterations assuming perfect phase correction.

As the Strehl ratio versus MSE plot assumed perfect phase correction on DM2, simulations were run to see if there was a resolution at which branch points started to dominate the degradation in the Strehl ratio. Hence the residual phase was examined for each turbulence condition tested at each apparent resolution. The residual phase was calculated as the phase of the field in the DM2 plane before compensation by DM2 minus the least-squares portion of the phase (irrotational portion). While all 4 turbulence conditions were tested, examples of the residual phase results for the lowest and highest turbulence conditions are shown in Figs. 4 and 5.

Note that once the number of subapertures across goes beyond $36-37$, the DM2 residual phase shown in Figs. 4 and 5 shows a significant decrease in the uniformity of the residual phase for both the lowest and highest turbulence conditions.

4. SIMULATION RESULTS

Finally, the Strehl ratio was used as the metric to determine the relative performance of the MCAO system using near field propagation at the various apparent resolution and turbulence conditions tested. DM1 was modelled as a segmented DM and DM2 was modelled as a continuous DM. The Strehl ratio versus σ_χ^2 plots do account for sensing branch points by using the least-squares principal-value best-of-8 residual phase technique of Venema and Schmidt[4] as shown in Fig. 7.

Note that for the 3 apparent resolutions in Fig. 6, taking the mean of the DM2 phase within the G-S loop before back propagating to the DM1 plane resulted in reducing the dynamic range of the phase (as shown on each respective phase color bar). By taking the mean of the DM2 phase within the G-S loop, the Strehl ratio

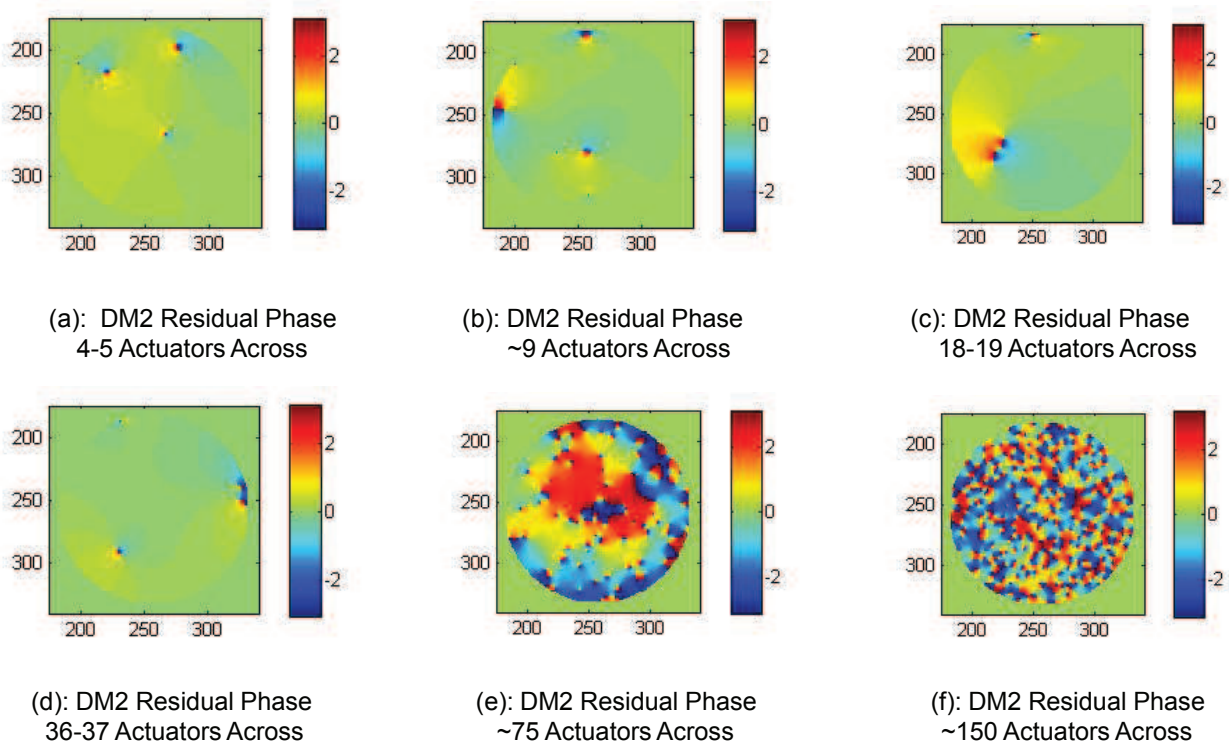

Figure 4. Least Squares Residual Phase Over Apparent Resolution Range, $r_0 = 0.3632$ m, $\sigma_\chi^2 = 0.1672$

could be improved $6 - 11$ percent for apparent resolutions with about $4 - 19$ actuators across. Beyond that (except at the lowest turbulence condition tested for 36 subapertures across), no benefit was noted in the Strehl ratio using that technique. That technique was not evaluated with noise added to the sensors.

As hinted at in the residual phase plots in Figs. 4 and 5, it appeared that 18 or 36 subapertures across (of the apparent resolutions simulated) would result in the highest Strehl ratio with it dropping off significantly after that due to the branch points. Figure 7 shows the best Strehl ratio (of the apparent resolutions tested) was achieved with $36 - 37$ subapertures across and that two DMs begin to show better performance than a single-DM system at $18 - 19$ subapertures across. However, at 75 and 150 subapertures across, the branch points seriously degrade the Strehl ratio. Note that the vertical axis on Fig. 7 (f) was extended down to 0 in order for the Strehl ratio (of about 0.01) to show up on the plot. Based on these results it appears that using 36 subapertures across provided the best tradeoff between more finely reshaping the amplitude and mitigating the generation of branch points. It is suspected that more branch points are generated by having subapertures sized about the size of the areas of the received field with zero intensity. Barchers[10] suggests that a $d/r_0 < 0.25$ is required to achieve a "significant degree of scintillation compensation." However, that threshold breaks down at the two highest apparent resolution cases tested for this research due to the huge increase in branch points; hence, maybe d/r_0 is not a sufficient metric to look at by itself. A tweak on the Barchers metric that holds up better for the simulation results of this research is to have $0.1 < d/r_0 < 0.5$ and 0.04 m $< d < 0.08$ m for significant scintillation compensation.

Visual inspection of the plot of the received irradiance and the residual phase at each apparent resolution confirmed the branch points appeared in areas of zero intensity. As the apparent resolution was increased, increasingly more branch points were evident. As the size of the subapertures got smaller, it appears the probability of that subaperture coinciding with a location of the received irradiance that had zero intensity was greatly increased. It was then postulated that if the irradiance could be redistributed to decrease the amount of the received field that had areas of zero intensity, a higher-resolution device could then be used on

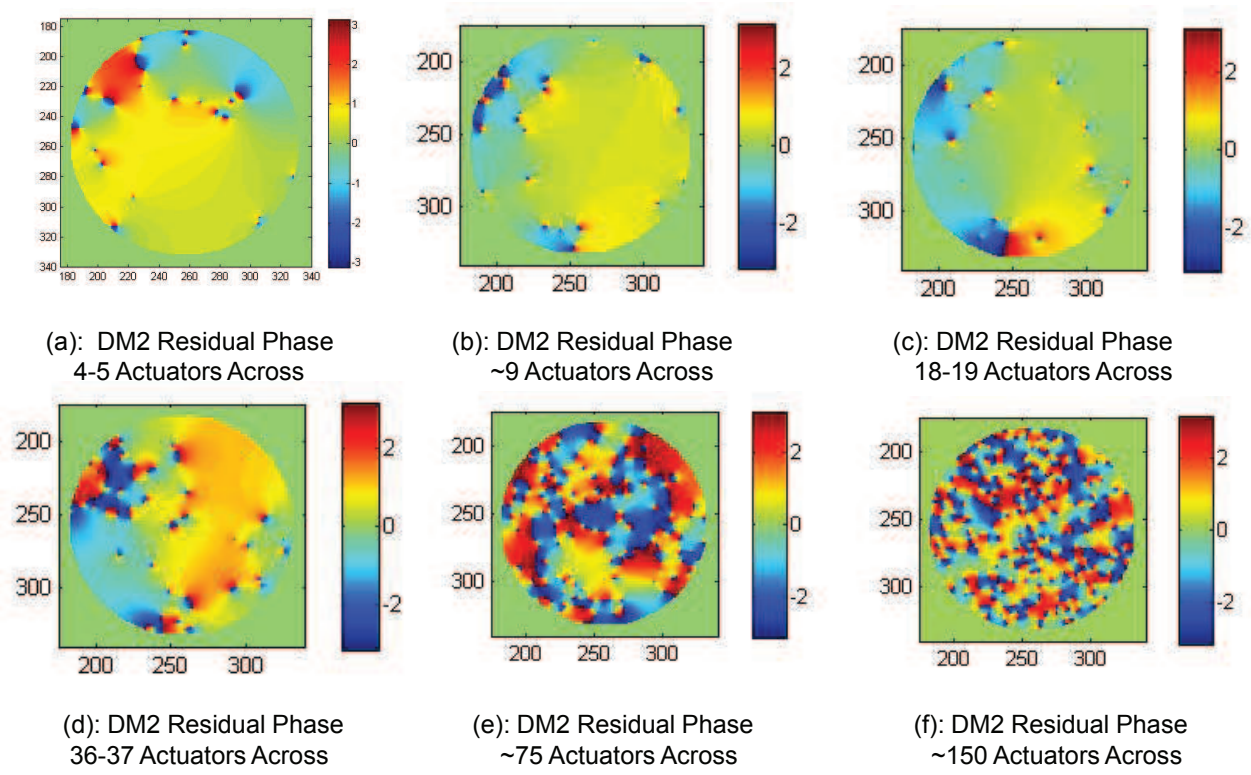

Figure 5. Least Squares Residual Phase Over Apparent Resolution Range, $r_0 = 0.1093$ m, $\sigma_\chi^2 = 1.2379$

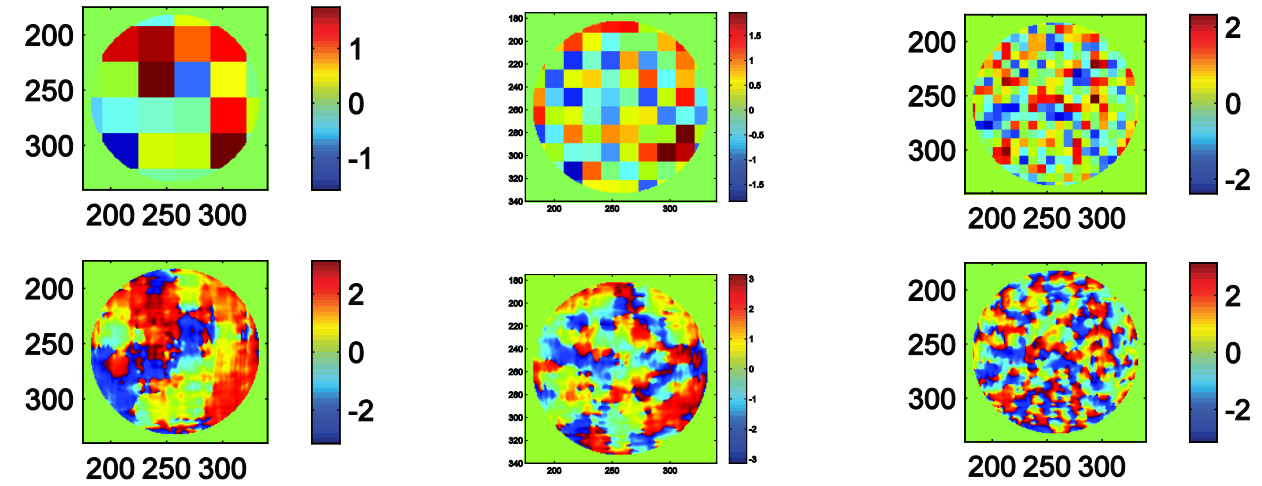

Figure 6. Pixellated and Unpixellated Phase for About 4, 9, and 18 Actuators Across

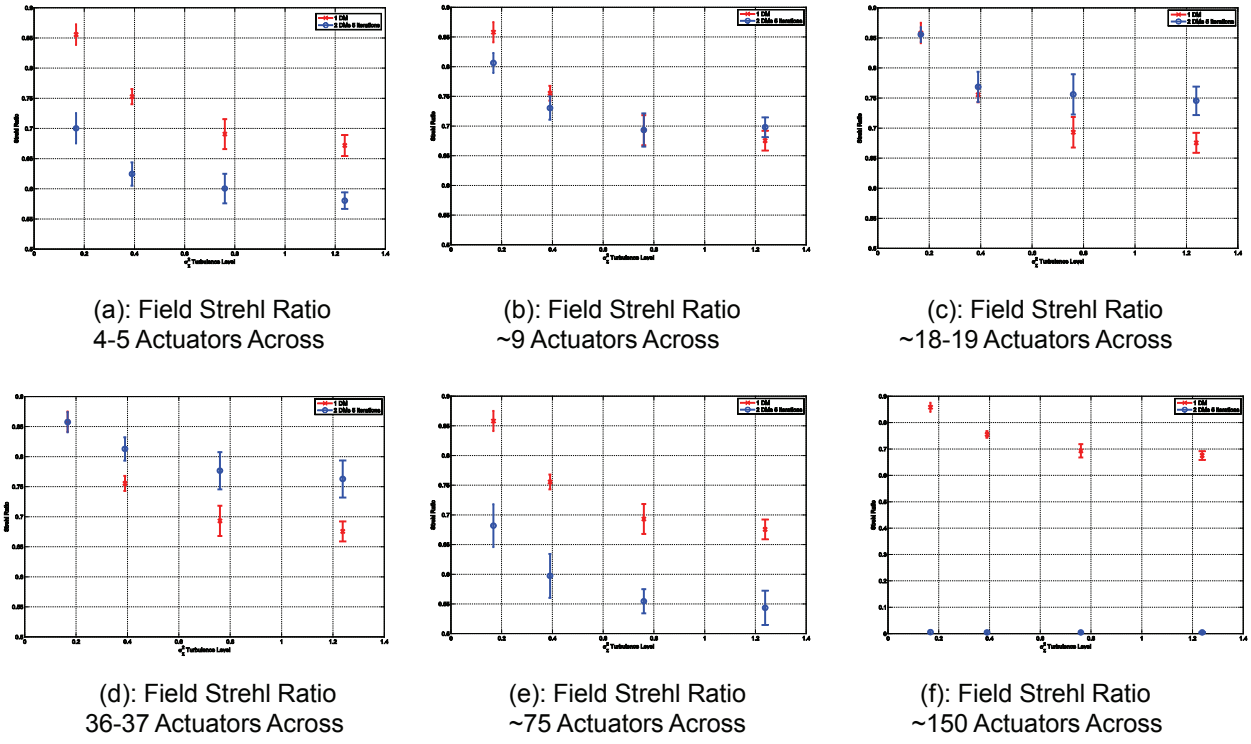

Figure 7. 1 DM and 2 DM Strehl Ratio Vs. σ_χ^2 Over Apparent Resolution Range (Mean of 10 Fields $\pm$ 1 σ); Note the Red "X" = Single DM and the Blue "O" = 2 DMs 5 GS Iterations

that reshaped field to further improve the Strehl ratio. Hence a simulation was run to cascade two DMs doing amplitude reshaping, with DM2 having a higher resolution than DM1, followed by a third DM doing a final phase flattening. As using 36 subapertures across gave the best results for the two-DM system simulation, the first segmented DM had 36 subapertures across, followed by a segmented DM with 75 subapertures across, and finally followed by a final continuous DM with 30 subapertures across.

In attempting to stay within the previous choice of five iterations, simulations were performed to determine if better Strehl ratios were obtained doing two iterations of amplitude reshaping at 36 subapertures across followed by three iterations at 75 subapertures across or vice versa. Doing three iterations of amplitude reshaping at 36 subapertures across followed by two iterations of amplitude reshaping at 75 subapertures across gave the better results. These results are shown in Fig. 8, with a comparison between one, two, and three DMs. Note that the 3-DM data were plotted slightly offset from the 2-DM turbulence conditions purely for display purposes so that the 1-sigma error bars could be visible. While doing three iterations at 36 subapertures across followed by two iterations at 150 subapertues across had over an order of magnitude improvement in the Strehl ratio of the two-DM system at five iterations and 150 subapertues across (about 0.01), the performance was still not better than that of a single-DM system due to presence of branch points (even with three DMs). A four-DM system with three stages of amplitude reshaping with successive increases in resolution was not investigated. Additionally, one more iteration was added for the three-DM case to determine if there was any benefit as Fig. 3 showed the most relative improvement in the Strehl ratio between iterations one to two and then from two to three. Note that if an additional iteration were used on the two-DM system, the improvement in the Strehl ratio would have been less than 0.01 mainly because there is a smaller relative improvement between iterations five and six. Similarly, an additional iteration in the three-DM system gave an improvement in the Strehl ratio of about 0.02.

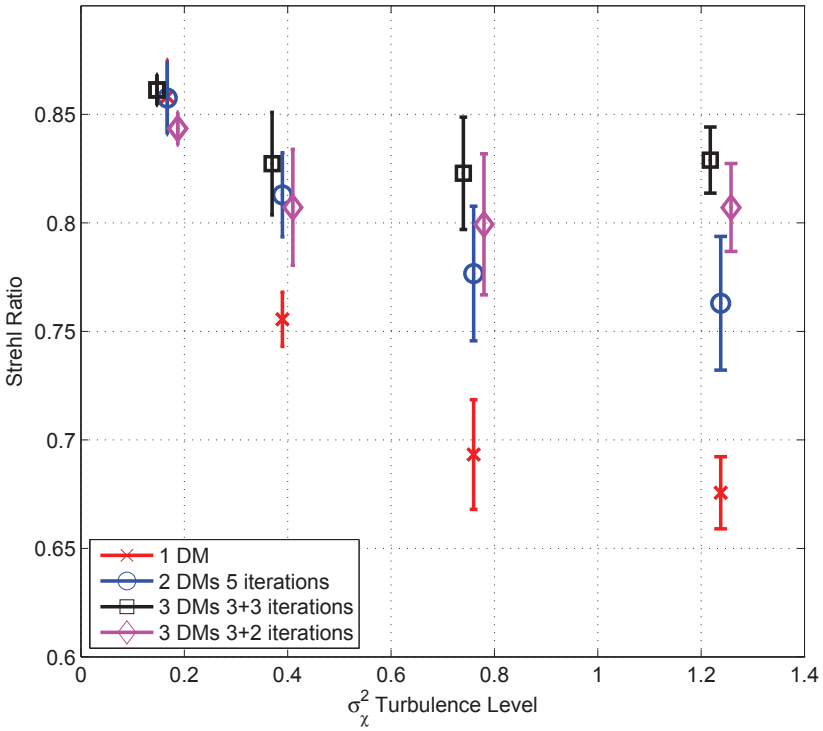

Figure 8. 1 DM, 2 DM, and 3 DM Strehl Ratio (Mean of 10 Fields $\pm$ 1σ) Versus σ_χ^2: The Single DM Case Uses a Modelled Continuous DM in the DM1 Plane With 30 $\times$ 30 Actuators and LSPV Phase Correction. The 2DM Case Uses 36-37 Subapertures Across Apparent Resolution on DM1 with LSPV Phase Correction on DM2 (Modelled as a Continuous DM) With 30 $\times$ 30 Actuators Using 5 G-S Iterations. The Pseudo 3DM System Uses 3 Iterations with 36 $\times$ 36 Actuators on DM1 Plus 2 and/or 3 Iterations with 75 $\times$ 75 Actuators on DM2 With a Modelled Continuous DM at the DM3 Plane With 30 $\times$ 30 Actuators

5. SUMMARY

By taking the mean of the DM2 phase within the G-S loop, the Strehl ratio could be improved $6-11$ percent for apparent resolutions with about $4-19$ actuators across. For these simulations, using about 36 subapertures across gave the best Strehl ratio in a two-DM MCAO system by balancing better control of the phase to achieve more uniform amplitude with the generation of branch points that resulted from using smaller subapertures. This was evidenced by the jump in nonuniformity of the DM2 residual phase as the number of subapertures was increased beyond 36 subapertures across at all turbulence conditions tested ($\sigma_\chi^2 = 0.17 - 1.24$). It was also demonstrated that using a mock three-DM system, cascading two DMs of increasingly higher resolution doing amplitude reshaping followed by a final DM for phase flattening can further improve the Strehl ratio using only five iterations of the G-S type algorithm.

As a phase-only (single degree of freedom) segmented DM with square subapertures and 100 percent fill factor was used in the DM1 plane of this simulated MCAO system, further research could be done using a segmented DM with subapertures of other shapes and more degrees of freedom. Additionally, it was not investigated whether taking the mean of the DM2 phase within the G-S loop was also effective in improving the Strehl ratio when noise was added to the system. Finally, a four-DM system with three stages of amplitude reshaping, with successive increases in resolution of each DM, was not investigated to see if the Strehl ratio could be improved further within a reasonable number of G-S iterations.

Acknowledgments

We would like to thank the Starfire Optical Range for sponsoring this research.

The views expressed in this paper are those of the authors and do not reflect the official policy or position of the United States Air Force, Department of Defense, or the United States Government.

REFERENCES

[1] Andrews, L. C. and Phillips, R. L., [*Laser Beam Propagation through Random Media*], SPIE Press, Bellingham, WA, second ed. (2005).

[2] Roggemann, M. C. and Lee, D. J., "Two-deformable-mirror concept for correcting scintillation effects in laser beam projection through the turbulent atmosphere," *Appl. Opt.* **37**, 4577–4585 (July 1998).

[3] Barchers, J. D. and Ellerbroek, B. L., "Improved compensation of turbulence-induced amplitude and phase distortions by means of multiple near-field phase adjustments," *J. Opt. Soc. Am. A* **18**, 399–411 (February 2001).

[4] Venema, T. M. and Schmidt, J. D., "Optical phase unwrapping in the presence of branch points," *Opt. Express* **16**, 6985–6998 (May 2008).

[5] Fried, D. L., "Branch point problem in adaptive optics," *J. Opt. Soc. Am. A* **15**, 2759–2768 (October 1998).

[6] Fried, D. L. and Vaughn, J. L., "Branch cuts in the phase function," *Appl. Opt.* **31**, 2865–2882 (20 May 1992).

[7] Gerchberg, R. W. and Saxton, W. O., "A practical algorithm for the determination of phase from image and diffraction plane pictures," *OPTIK* **35**(2), 237–246 (1972).

[8] Fienup, J. R., "Iterative method applied to image reconstruction and to computer-generated holograms," *Opt. Engineering* **19**, 297–305 (May/June 1980).

[9] Fienup, J. R., "Phase retrieval algorithms: a comparison," *Appl. Opt.* **21**, 2758–2769 (August 1982).

[10] Barchers, J. D., "Evaluation of the impact of finite-resolution effects on scintillation compensation using two deformable mirrors," *J. Opt. Soc. Am. A* **18**, 3098–3109 (December 2001).

[11] Barchers, J. D., Fried, D. L., Link, D. J., Tyler, G. A., Moretti, W., Brennan, T. J., and Fugate, R. Q., "The performance of wavefront sensors in strong scintillation," *SPIE* **4839**, 217–227 (February 2003).

[12] Roggemann, M. C. and Welsh, B., [*Imaging Through Turbulence*], CRC Press, New York, NY (1996).

[13] Schmidt, J. D., "AFIT lecture notes: Wave optics I class," (2007).

[14] Welsh, B. M., "Fourier-series-based atmospheric phase screen generator for simulating anisoplanatic geometries and temporal evolution," *SPIE* **3125**, 327 (April 1997).

[15] Magee, E. P., "Mission research corporation presentation: Phase screens for long time series wave optics simulations," (May 2003).

[16] Schmidt, J. D., "AFIT lecture notes: Imaging through turbulence class," (2007).

[17] Goodman, J. W., [*Introduction to Fourier Optics*], Roberts & Company, Englewood, CO, third ed. (2005).

[18] Sklar, B., [*Digital Communications Fundamentals and Applications*], Prentice Hall PTR, Upper Saddle River, New Jersey, second ed. (2001).

[19] Martin, J. M. and Flatté, S. M., "Simulation of point-source scintillation through three-dimensional random media," *J. Opt. Soc. Am. A* **7**, 838 – 847 (May 1990).

[20] Lukin, V. P. and Fortes, B. V., [*Adaptive Beaming and Imaging in the Turbulent Atmosphere*], SPIE Press, New York, NY (2002).

[21] Jagourel, P. and Gaffard, J.-P., "Adaptive optics components in laserdot," *SPIE* **1543**, 76–86 (July 1991).

[22] Ealey, M. A. and Wellman, J. A., "Deformable mirrors: Design fundamentals, key performance specifications, and parametric trades," *SPIE* **1543**, 36–51 (July 1991).

DISTRIBUTION LIST

DTIC/OCP
8725 John J. Kingman Rd, Suite 0944
Ft Belvoir, VA 22060-6218 1 cy

AFRL/RVIL
Kirtland AFB, NM 87117-5776 2 cy

Patrick Kelly
Official Record Copy
AFRL/RDSA 1 cy

This page intentionally left blank.